Anal. Chem. **2000,** *72,* 2737−2740

Mobility Labeling for Parallel CID of Ion Mixtures

Cherokee S. Hoaglund-Hyzer, Jianwei Li, and David E. Clemmer*

Department of Chemistry, Indiana University, Bloomington Indiana 47405

An ion mobility/mass spectrometry technique has been developed to record collision-induced dissociation patterns for multiple ions in a parallel fashion. In this approach, a mixture of ions is separated in a drift tube on the basis of differences in mobilities through a buffer gas. As the ions exit the drift tube, they are accelerated into a collision cell and the ensuing fragment ions are dispersed by differences in mass-to-charge (m/z) ratios in a time-of-flight mass spectrometer. Fragment ions that are formed in the collision cell have drift times that are coincident with their antecedent parent ions, allowing the origin of all fragments formed from the mixture of ions to be determined. The approach is demonstrated by examining fragmentation patterns of the $[M + H]^+$ parent and a series of a-, b-, and y-type fragments of [D-Ala^{2,3}]methionine enkephalin.

The use of fragmentation patterns to infer primary molecular structure is common to many mass spectrometry (MS)-based techniques. Extensive mass spectral databases and search/characterization algorithms for ions produced by electron impact have a long history;[1] recently, large biomolecular databases for characterization of proteins have been compiled.[2] Multiple stages of MS are useful for elucidating structures of unknowns since each fragment ion originates from a precursor with a defined mass-to-charge (m/z) ratio. However, initial m/z selection is an inherently inefficient process since other m/z ions from the sample are discarded. Methods that utilize direct dissociation of mixtures of ions are more efficient, but structural assignments are less definitive because daughter ions are not uniquely associated with parents. In this paper, we introduce a method that allows fragments generated from a mixture of ions to be assigned to appropriate precursors. The approach is based on an ion mobility/time-of-flight mass spectrometry technique that allows a mixture of ions to be separated prior to being dispersed into a mass spectrometer for m/z analysis.[3] The unique mobility of an individual ion in the mixture is used as a label for determining the origin of fragments.

Key to this approach is that the microsecond ion flight times (in the evacuated mass spectrometer) are substantially shorter than millisecond drift times (through the high-pressure mobility instrument). This allows flight time distributions to be recorded within individual drift time windows; thus, mobilities and m/z ratios for mixtures of ions can be determined in a single experimental sequence.[3] By introducing a collision cell between the ion mobility and time-of-flight instruments, it is possible to create fragments that are labeled according to the mobility of the precursor ion from which they originate. We demonstrate the approach by examining collision-induced dissociation (CID) patterns of the $[M + H]^+$ parent and a series of a-, b-, and y-type fragments of [D-Ala^{2,3}]methionine enkephalin that were generated prior to mobility separation. Dissociation of these sequence-related fragment ions yields many fragments having identical m/z ratios. The coincidence in drift times between each fragment (formed in the collision cell) and its corresponding parent allows the origins of identical m/z species to be determined.

EXPERIMENTAL SECTION

The operating principles of ion mobility techniques[4] and recent applications to studies of biomolecular ions[5] have been presented previously. Only a brief description of the ion mobility/collision cell/time-of-flight method is given here. Figure 1 shows a schematic diagram of the instrument components. The ion trap and injected-ion drift tube portions have been described previously[6] and are situated in a large vacuum chamber that is pumped by two Edwards ISO-250 diffusion pumps. The collision cell and time-of-flight mass spectrometer are housed in separate adjoining chambers that are each pumped by an Edwards ISO-160 diffusion pump. The time-of-flight mass spectrometer is a simple linear instrument that is situated orthogonally to the axis of the ion beam.[7]

(1) For recent discussions, see: McLafferty, F. W.; Staffer, D. A.; Loh, S. Y.; Wesdemiotis, C. *J. Am. Soc. Mass Spectrom.* **1999**, *10*, 1229. McLafferty, F. W.; Zhang, M.-Y.; Stauffer, D. B.; Loh, S. Y. *J. Am. Soc. Mass Spectrom.* **1998**, *9*, 92.

(2) For recent discussions of protein databases and search algorithms, see the following papers and references therein: Eng, J. K.; McCormack, A. L.; Yates, J. R., III. *J. Am. Soc. Mass Spectrom.* **1994**, *5*, 976. Yates, J. R., III.; Eng, J. K.; Clauser, K. R.; Burlingame, A. L. *J. Am. Soc. Mass Spectrom.* **1996**, *7*, 1089. Jensen, O. N.; Podtelejnikov, A. V.; Mann, M. *Anal. Chem.* **1997**, *69*, 4741. Reiber, D. C.; Grover, T. A.; Brown, R. S. *Anal. Chem.* **1998**, *70*, 673. Clauser, K. R.; Baker, P.; Burlingame, A. L. *Anal. Chem.* **1999**, *71*, 2871.

(3) Hoaglund, C. S.; Valentine, S. J.; Sporleder, C. R.; Reilly, J. P.; Clemmer, D. E. *Anal. Chem.* **1998**, *70*, 2236.

(4) Tou, J. C.; Boggs, G. U. *Anal. Chem.* **1976**, *48*, 351. Hagen, D. F. *Anal. Chem.* **1979**, *51*, 870. Karpas, Z.; Stimac, Rappaport, Z. *Int. J. Mass Spectrom. Ion Processes* **1988**, *83*, 163. St. Louis, R. H.; Hill, H. H. *Crit Rev. Anal. Chem.* **1990**, *21*, 321. Hill, H. H.; Siems, W. F.; St. Louis, R. H.; McMinn, D. G. *Anal. Chem.* **1990**, *62*, 1201A. von Helden, G.; Hsu, M.-T.; Kemper, P. R.; Bowers, M. T. *J. Chem. Phys.* **1991**, *95*, 3835. Jarrold, M. F. *J. Phys. Chem.* **1995**, *99*, 11.

(5) For recent reviews of ion mobility studies of biomolecules, see: Hoaglund-Hyzer, C. S.; Counterman, A. E.; Clemmer, D. E. *Chem. Rev.* **1999**, *99*, 3037. Clemmer, D. E.; Jarrold, M. F. *J. Mass Spectrom.* **1997**, *32*, 577. Liu, Y.; Valentine, S. J.; Counterman, A. E.; Hoaglund, C. S.; Clemmer, D. E. *Anal. Chem.* **1997**, *69*, 728A.

(6) Hoaglund, C. S.; Valentine, S. J.; Clemmer, D. E. *Anal. Chem.* **1997**, *69*, 4156.

(7) Henderson, S. C.; Valentine, S. J.; Counterman, A. E.; Clemmer, D. E. *Anal. Chem.* **1999**, *71*, 291.

10.1021/ac0000170 CCC: $19.00
Published on Web 05/11/2000

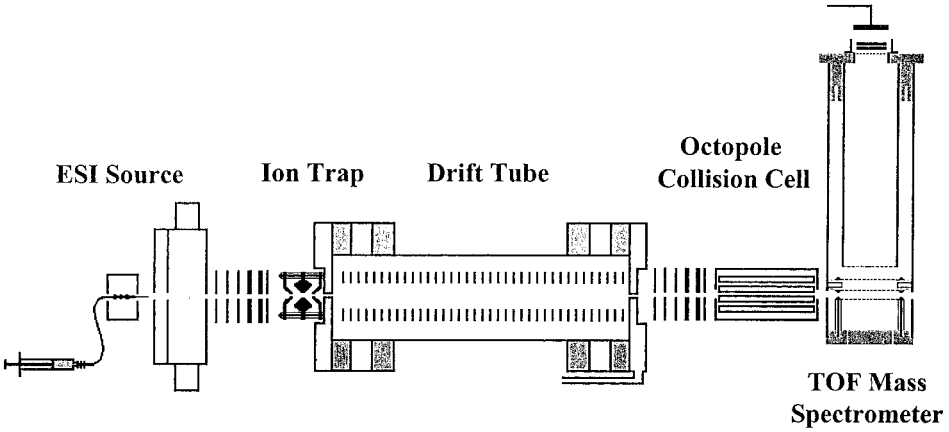

Figure 1. Schematic diagram of the experimental ion mobility/collision cell/TOFMS instrument used for mobility labeling CID experiments.

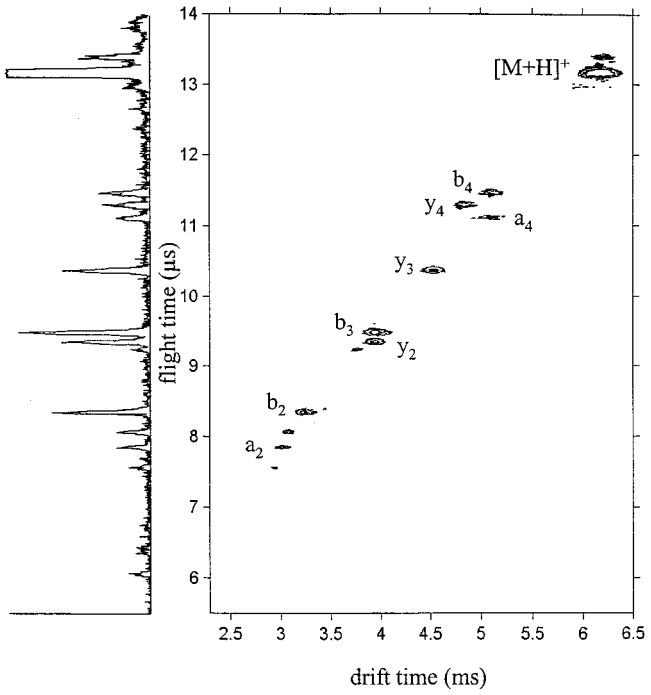

Figure 2. Two-dimensional contour plot of nested drift (flight) time data for a mixture of ions formed from electrosprayed [D-Ala^{2,3}]-methionine enkephalin. These data were recorded with no gas in the octopole collision cell. The contours are shown on a 10-point scale; this removes all features that contain fewer than 10 ion counts. The distribution includes a series of a-, b-, and y-type fragment ions that are formed upon high-energy injection into the drift tube (see text). The drift time axis has been normalized to a helium pressure of 2.70 Torr. Also shown (left) is the time-of-flight mass spectrum obtained by integrating the flight time data over the drift time range. (Data are plotted on a normalized intensity scale so that peak heights can be compared directly with the data in Figure 3.) The resolving power along the flight time axis is typically 200 ($m/\Delta m$ of a peak for a singly charged ion, where Δm is determined at half-maximum). Along the drift time axis, the resolving power ($t/\Delta t$, where Δt is determined at half-maximum) is between 20 and 30, for all peaks.

The experimental sequence that is used to label fragment ions produced by collision-induced dissociation with the gas cell is as follows. Briefly, ions were formed by electrospraying[8] a 0.25 mg mL^{-1} solution of [D-Ala^{2,3}]methionine enkephalin (Sigma 98% purity) in 49:49:2 water/acetonitrile/acetic acid into a differentially pumped desolvation region. Ions are extracted into the main vacuum chamber ($\sim 5 \times 10^{-5}$ Torr) and focused into an ion trap ($\sim 5 \times 10^{-4}$ Torr) where they are accumulated for 100 ms and then injected as a short pulse (1.0 μs) into a 53.5-cm-long drift tube containing ~2.5 Torr of He buffer gas. The ion packet drifts through the gas under the influence of a weak uniform electric field (9.35 V cm^{-1}) and different ions are separated on the basis of differences in their mobilities.[4,5] Ion injection conditions were chosen to favor formation of some fragment ions at the entrance of the drift tube.[6,9]

Ions that exit the drift tube are focused into a 22.9-cm-long octopole collision cell. The octopole is operated at 1.7 MHz and ~540 V (peak to peak). For CID experiments, the gas cell is filled with a target gas (usually zero grade argon). The background chamber pressure during CID experiments is $\sim 3 \times 10^{-6}$ Torr; we estimate that the pressure within the cell is $\sim 5 \times 10^{-4}$ Torr. Parent and fragment ions exit the collision cell directly into the source region of the time-of-flight mass spectrometer (typically 2×10^{-6} Torr) where high-voltage, high-frequency pulses, that are synchronous with the initial injection pulse, are used to initiate flight time measurements. Flight times are recorded within individual drift time windows using a nested data acquisition system.[3,7] The time-of-flight tube is 56.5 cm long, and a four-grid source is used to pulse ions into this instrument and for space- and velocity-focusing.[10]

The arrival time of a packet of ions at the detector is a composite of the drift time, flight time, and the time required to travel through other portions of the instrument. When the octopole is evacuated, differences between arrival times and drift times are relatively small, ~120−180 μs for the ions studied here. Although we have not measured the pressure in the gas cell directly, we have maintained conditions where arrival times for mobility-separated precursor ions are within 20 μs of values recorded when no argon is present.

RESULTS AND DISCUSSION

Figure 2 shows a two-dimensional contour plot of a nested drift (flight) time distribution for electrosprayed [D-Ala^{2,3}]methionine enkephalin. These data were recorded upon injecting ions into

(8) Fenn, J. B.; Mann, M.; Meng, C. K.; Wong, S. F.; Whitehouse, C. M. *Science* **1989**, *246*, 64.

(9) Liu, Y.; Clemmer, D. E. *Anal. Chem.* **1997**, *69*, 2504.

(10) Colby, S. M.; Reilly, J. P. *Anal. Chem.* **1996**, *68*, 1419.

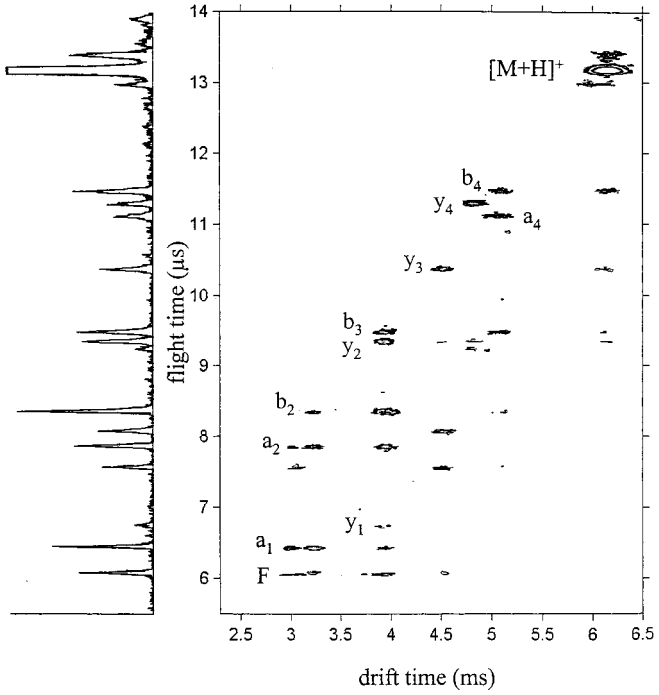

Figure 3. Two-dimensional contour plot of drift (flight) time data recorded when ~5 × 10^{-4} Torr of argon is added to the octopole collision cell. Fragment ions formed in the collision cell are observed at the drift times of the antecedent parent ions. All other conditions are the same as in Figure 2.

the drift tube at an injection energy of 100 eV (for singly protonated ions). As discussed previously,[9,11,12] when ions are injected from the low-pressure vacuum chamber into the drift tube, they undergo a rapid heating/cooling cycle; initial collisions of ions with the buffer gas thermalize their kinetic energy and subsequent collisions cool them to the buffer gas temperature. Figure 2 shows that a fraction of $[M + H]^+$ parent ions formed by electrospray ionization have dissociated to series of a-, b-, and y-type fragment ions.[13,14] A series of studies of fragmentation patterns as a function of energy (without the ion trap) suggests that fragments are formed upon injection into the drift tube; however, we cannot rule out the possibility that a small fraction of the fragments are formed in the ion trap prior to injection. With the exception of the b_4/a_4 and b_3/y_2 pairs, all fragments are at least partially separated due to differences in mobilities. Also shown in Figure 2 is a plot of the time-of-flight mass spectrum—obtained by integrating ion intensity across the drift time dimension. The largest fragment peaks are associated with the b_3, b_2, y_3 and y_2 fragment ions.

Figure 3 shows a contour plot and integrated mass spectrum for a nested drift (flight) time distribution when ~5 × 10^{-4} Torr of argon is added to the octopole collision cell. With the target gas, two features are apparent in the data. The integrated mass spectrum shows that the relative magnitudes of fragment peaks are substantially different from the mass spectrum in Figure 2. In particular, smaller fragment ions are more abundant (e.g., m/z < 250); an increase in intensities of small fragment peaks is consistent with formation of fragments in the octopole collision cell. The two-dimensional plot of data in Figure 3 shows that many additional peaks are present (compared with Figure 2). Analysis of the time-of-flight dimension for these peaks shows that the new peaks can also be assigned to expected fragments of the [D-Ala[2,3]]-methionine enkephalin peptide. For example, at a flight time of 7.85 μs, we observe three clearly resolved peaks having drift times of 3.01, 3.24, and 3.94 ms. The 7.85-μs flight time of all of these peaks clearly indicates that all are a_2 ions. The drift times of these features are essentially identical to the 3.01-, 3.20-, and 3.94-ms drift times recorded for the a_2, b_2, and unresolved b_3/y_2 pair observed when no collision gas was added to the gas cell (Figure 2). The appearance of the a_2 ion at 3.01 ms in Figure 3 arises from the original injected-ion fragmentation process (discussed above, Figure 2); however, the 3.20- and 3.94-ms drift times indicate that these a_2 ions must arise from dissociation of the b_2 and unresolved b_3/y_2 pair, respectively. Every fragment in Figure 3 either corresponds to a precursor (that did not undergo CID in the gas cell) or can be assigned as a CID product that is correlated with a precursor ion having a specific mobility. These data effectively illustrate the use of the mobility as a label for parallel sequencing of the ion mixture—even when many of the fragment ions that are produced from different parent ions have identical m/z ratios.

Figure 4 shows example plots of several mass spectra on a m/z scale. The different spectra were obtained by taking slices through the data at specific drift times. Several interesting features are observed. The region of drift times in Figures 2 and 3 from ~4.8 to 5.1 ms shows three peaks, corresponding to the b_4, y_4, and a_4 ions, centered at 5.08, 4.81, and 5.08 ms, respectively. The virtually identical drift times and peak shapes associated with the b_4/a_4 pair prohibit us from discerning the fraction of y_2 and b_2 ions that originate from the individual precursors. Thus, the mass spectral slice in Figure 4 may contain fragments from both precursor ions. We have attempted to discriminate between the sources of y_2 and b_2 ions by taking mass spectral slices at other drift times across the peaks; however, no discernible differences are observed. On the other hand, the 0.27-ms shift to shorter drift times associated with the y_4 ion is enough to unambiguously assign the AAF and b_3 fragment peaks centered at a drift time of 4.81 ms to the y_4 parent (and not the nearby a_4 and b_4 peaks). Similarly, the fragmentation pattern of the y_3 precursor is readily resolved, while differences in mobility for the b_3/y_2 pair are not sufficient to definitively distinguish which parent ions are associated with the fragments observed at 3.94 ms.

A final note is that information about the relative fragmentation efficiencies of the different precursor ions is readily accessible from these data. For example, the mass spectral slices shown in Figure 4 show that collision-induced dissociation of the y_3 ion is relatively efficient. About 70% of parent y_3 undergoes dissociation in the gas cell, while only ~30% of the y_4 ion dissociates. The use of an octopole collision cell should allow efficient collection of parent and fragment ions in these studies—an important consideration for determining fragmentation efficiency.

(11) Jarrold, M. F.; Honea, E. C. *J. Phys. Chem.* **1991**, *95*, 9181.
(12) Jarrold, M. F.; Constant, V. A. *Phys. Rev. Lett.* **1991**, *67*, 2994.
(13) Fragment nomenclature is consistent with that described by: Biemann, K. *Biomed. Environ. Mass Spectrom.* **1988**, *16*, 99. Biemann, K. *Methods Enzymol.* **1990**, *193*, 886.
(14) Flight times for peaks were converted to m/z ratios using a standard calibration. Assignments were made by comparison of experimental m/z ratios with values from the MSProduct program from Protein Prospector, http://prospector.ucsf.edu.

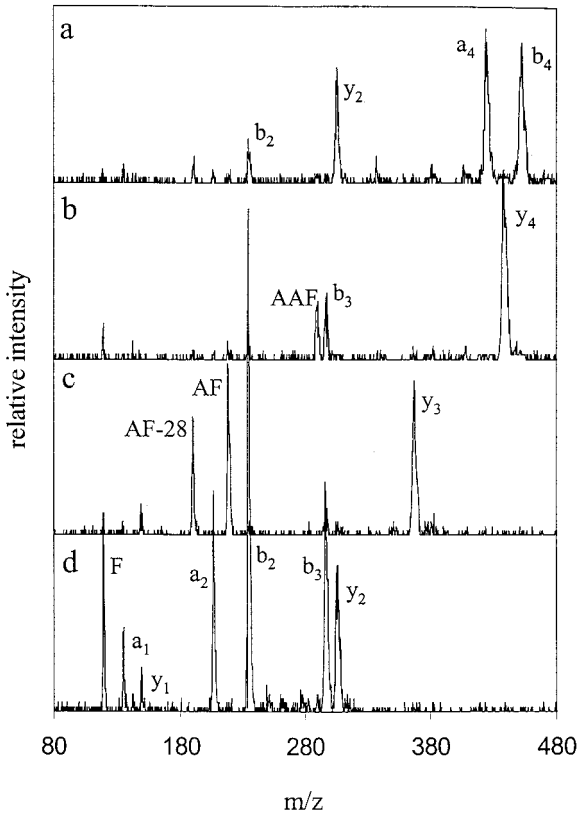

Figure 4. Mass spectral slices taken at specific drift times across the two-dimensional data set shown in Figure 3. These slices are obtained by summing the individual flight time spectra for ~5 drift time windows across the parent ion peak. Part a shows the mass spectrum obtained for a drift time center of 5.08 ms. The fragment peaks arise from dissociation of a_4 and b_4 ions that were not resolved along the drift time axis. Part b shows a slice centered at 4.81 ms. In this case, all fragment ions arise from dissociation of the resolved y_4 ion. Part c shows a slice centered at 4.49 ms corresponding to fragmentation of the resolved y_3 ion. Part d shows a slice centered at 3.94 ms. Fragments in this slice may arise from either (or both) of the unresolved y_3 and b_3 ions.

SUMMARY AND CONCLUSIONS

Nested ion mobility/time-of-flight techniques[3] have been extended as a means of obtaining ion fragmentation patterns for mixtures of ions in a parallel fashion. The approach utilizes an octopole collision cell situated between the drift and flight tube portions of an existing instrument. A key feature of these experiments is that the millisecond ion drift times in the mobility instrument are substantially longer than the time required for ions to dissociate in the collision cell (and flight times in the time-of-flight mass spectrometer). In this case, the coincidence in drift times of fragment ions generated by CID in the octopole gas cell with the antecedent parent ions can be used to establish the origin of peaks. In cases where the ion mobility separation has fully resolved peaks, unambiguous assignments of parent and fragment peaks can be made. In the present study, two pairs of peaks (the b_4/a_4 and b_3/y_2 pairs) were not resolved on the basis of differences in their mobilities; in these cases, fragment peaks may have arisen from either (or both) of the possible parents.

The present experimental configuration is limited because we have utilized a low-resolution injected-ion drift tube configuration; analysis of peaks in Figures 2 and 3 along the mobility dimension show typical resolving powers of ~20−30. Recently, several groups have developed high-resolution drift tubes that routinely provide resolving powers in excess of 100 for singly charged ions;[15−17] substantially higher values have been reported for multiply charged ions.[16,18] We are currently developing a parallel CID instrument that utilizes a high-resolution drift tube with a high-resolution reflectron geometry time-of-flight mass spectrometer; we expect that parallel CID analysis of reasonably large ion mixtures (containing ~300−600 components) will be feasible.

Finally, it is worthwhile to note that an important application of ion mobility methods has been the ability to resolve and characterize different conformations of peptides and proteins that are stable during the millisecond drift times in the mobility instrument.[19] An application of parallel CID methods will be to investigate the possibility that different fragment ions may arise for different conformations—a project that is also underway in our laboratory.

ACKNOWLEDGMENT

This work is supported by a grant from the NIH (1RO1GM-59145-01).

Received for review January 4, 2000. Accepted March 31, 2000.

AC0000170

(15) Dugourd, P.; Hudgins, R. R.; Clemmer, D. E.; Jarrold, M. F. *Rev. Sci. Instrum.* **1997**, *68*, 1122.
(16) Wu, C.; Siems, W. F.; Asbury, G. R.; Hill, H. H., Jr. *Anal. Chem.* **1998**, *70*, 4929.
(17) Counterman, A. E.; Valentine, S. J.; Srebalus, C. A.; Henderson, S. C.; Hoaglund, C. S.; Clemmer, D. E. *J. Am. Soc. Mass Spectrom.* **1998**, *9*, 743.
(18) Srebalus, C. A.; Li, J.; Marshall, W. S.; Clemmer, D. E. *Anal. Chem.* **1999**, *71*, 3918.
(19) Clemmer, D. E.; Hudgins, R. R.; Jarrold, M. F. *J. Am. Chem. Soc.* **1995**, *117*, 10141.